

## **DYNAMIC BEHAVIOR OF AN AXIALLY MOVING WIDE WEB**

AGNIESZKA CEDROWSKA

*Technical University of Łódź, Faculty of Mechanical Engineering, PhD student*

KRZYSZTOF MARYNOWSKI

*Technical University of Łódź, Department of Machines Dynamics*

*e-mail: kmarynow@p.lodz.pl*

Theoretical and experimental dynamic analysis of an axially moving wide composite web is presented in this paper. The mathematical model of the system under consideration has the form of a differential equation with partial derivatives. The approximate solution using the extended Galerkin method has been determined in this work. Dynamic analysis allowed one to determine the natural frequency of bending and torsional vibrations of the web. Experimental investigations of dynamic behavior of the axially moving web was performed on a laboratory stand in the form of belt transmission. The experimental verification of numerical studies concerned the lowest frequencies of bending and torsional vibrations. The fundamental frequency of bending vibration was determined numerically with the greatest accuracy.

*Key words:* axially moving plate, dynamic analysis, experimental verification

### **1. Introduction**

Axially moving flat objects at high speeds can be found in many different technical facilities. These include band saws, paper webs during production, processing and printing, textile webs during production and processing, tubes transporting fluids, conveyor belts and flat objects moving at high speeds in space. In all of these various technical applications, typically one tends to maximize the transport speed in order to increase productivity and optimize investment and operating costs of such, sometimes very expensive and complicated, equipment. An obstacle in the realization of these aspirations is very common dynamic behavior of axially moving systems.

For example, the maximum transport speed with which the moving paper web during manufacturing and processing currently reach 50 m/s. Under certain conditions, such high-transport speed can lead to resonance vibrations or flutter instability of the web. Such behavior can cause warping or breaking of the moving web. Changes in web tension due to vibration may become a cause of changes in the thickness of the produced paper.

The studies of dynamic behavior of axially moving systems began 60 years ago. Initial works included the analysis of lateral vibration of a moving string (Sack, 1954). Since that time, seen a lot of researchers focused much attention to this field of knowledge. Looking at the literature, one can find that over time the object being studied became increasingly complex. Starting from axially moving one-dimensional systems (strings, threads) through beam systems, now the effort is placed at axially moving plate systems.

The first paper in which dynamics of the plate model of a band saw blade was analyzed was authored by Ulsoy and Mote (1982). The partial differential equation of motion was discretized with the Ritz method. Approximate boundary conditions on free edges of the plate were taken into consideration, which – as pointed out in some further studies – affects fundamentally accuracy of the solution, especially in the overcritical range of the plate motion. The

fundamental study showing vibration characteristics and results of investigations of stability of axially moving elastic plates within the linear theory was published by Lin (1997). Vibrations of a two-dimensional, axially moving isotropic plate with two simply supported ends and two free ends were analyzed. On the basis of the Mindlin-Reissner plate theory, Wang (1999) presented a description of the finite element for an axially moving thin plate. It was found that it was possible to determine not only the critical transport speed of the web but a distribution of normal stresses and shear stresses in the moving web with such finite elements. Another formulation of the finite element was presented by Kim *et al.* (2003), where equations of the modal finite element within the frequency domain were formulated on the basis of the Kantorowitz method.

The literature, especially related to transverse vibrations of viscoelastic plates, is rather limited. A two-dimensional rheological element was applied in dynamic investigations of axially moving systems by Marynowski (2006, 2008). In the literature, one can also find works in which one-dimensional rheological models were used to describe properties of the axially moving material. The paper by Fung *et al.* (1997) was the first one where transverse vibrations of a viscoelastic moving belt represented by the spring model were investigated. Nonlinear dynamics of an axially accelerating viscoelastic beam was investigated by Chen *et al.* (2004) and Yang and Chen (2005). In those papers, the beam material was described with the Kelvin-Voigt model. Regular and chaotic vibrations of an axially moving viscoelastic beam subjected to tension variations were studied by Marynowski and Kapitaniak (2007) and Marynowski (2008). In those works, two different rheological models, namely: two-parameter Kelvin-Voigt model and three-parameter Zener model, were applied.

Two studies (Hatami *et al.*, 2007) and (Hatami *et al.*, 2008) devoted to free vibrations of axially moving multi-span composite plates and a viscoelastic Navier-type plate. In those papers, an exact finite strip method was developed for dynamic analysis of axially moving elastic and viscoelastic plates. The exact stiffness matrix of a finite strip of the plate was defined in the frequency domain. By joining these matrices, the global stiffness matrix of the whole plate was obtained. In the case of the viscoelastic plate with all simply supported edges, the eigenvalues of the global stiffness matrix have the form of complex numbers.

Recently, in the study by Marynowski (2010), the viscoelastic theory was applied to the axially moving Levy-type plate with two simply supported and two free edges. On the basis of the elastic-viscoelastic equivalence, a linear mathematical model in the form of the equilibrium state equation of the moving plate was derived in the complex frequency domain. The effects of transport speed and relaxation times modeled with two-parameter Kelvin-Voigt and three-parameter Zener rheological models on the dynamic behavior of the axially moving plate were presented.

This paper presents dynamic analysis of an axially moving wide web. The second section presents the non-linear mathematical model of the moving web and its solution using the extended Galerkin method. The experimental stand built to study the dynamic behavior of axially moving systems is shown in third section. That section also presents the results of numerical analysis and their experimental verification. The final conclusions and remarks are placed in forth section.

## 2. Mathematical model of the moving web

A thin plate of the length  $l$ , width  $b$  and thickness  $h$  is considered. The plate moves along the longitudinal direction  $x$  at the constant velocity  $c$ . The co-ordinate system and the geometry are shown in Fig. 1.

The forces that act on a small element of the plate  $dA$  are shown in Fig. 1 as well. The partial differential equation resulting from Hamilton's principle for transverse motion of the

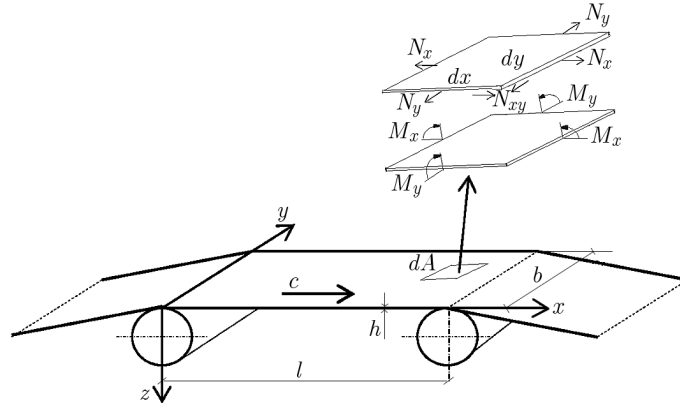


Fig. 1. Axially moving plate and internal forces acting on an infinitely small element  $dA$

two-dimensional axially moving plate was derived by Marynowski (2008) and has the following form

$$\begin{aligned} \rho h \left( \frac{\partial^2 \bar{w}}{\partial t^2} + 2c \frac{\partial^2 \bar{w}}{\partial x \partial t} + c^2 \frac{\partial^2 \bar{w}}{\partial x^2} \right) - \frac{\partial(N_x \bar{w},_x)}{\partial x} - \frac{\partial(N_y \bar{w},_y)}{\partial y} \\ - \frac{\partial(N_{xy} \bar{w},_x)}{\partial y} - \frac{\partial(N_{xy} \bar{w},_y)}{\partial x} + D \left( \frac{\partial^4 \bar{w}}{\partial x^4} + 2 \frac{\partial^4 \bar{w}}{\partial x^2 \partial y^2} + \frac{\partial^4 \bar{w}}{\partial y^4} \right) = 0 \end{aligned} \quad (2.1)$$

where  $r$  is the mass density,  $h$  – thickness,  $\bar{w}$  – transverse displacement of the plate,  $D$  – plate stiffness;  $N_x, N_y, N_{xy}$  – in-plane forces per unit length.

Equation (2.1) can be transposed to a dimensionless form using the following terms

$$\begin{aligned} z = \frac{\bar{w}}{h} \quad \mu = \frac{x}{l} \quad \varphi = \frac{y}{l} \quad r = \frac{b}{l} \quad \Omega = \sqrt{\frac{D}{h\rho l^4}} \\ s = \frac{c}{\Omega l} \quad \tau = \Omega t \quad n_x = \frac{N_x l^2}{D} \quad n_y = \frac{N_y l^2}{D} \quad n_{xy} = \frac{N_{xy} l^2}{D} \end{aligned} \quad (2.2)$$

where  $\Omega$  denotes the angular frequency,  $\tau$  is the dimensionless time.

Then the dimensionless equation of motion has the form

$$\begin{aligned} z_{,\mu\mu\mu\mu} + \frac{2}{r^2} z_{,\mu\mu\varphi\varphi} + \frac{1}{r^4} z_{,\varphi\varphi\varphi\varphi} + z_{,\tau\tau} + 2s z_{,\mu\tau} + s^2 z_{,\mu\mu} \\ - (n_x z_{,\mu})_{,\mu} - \frac{1}{r} (n_{xy} z_{,\varphi})_{,\mu} - \frac{1}{r} (n_{xy} z_{,\mu})_{,\varphi} - \frac{1}{r} (n_y z_{,\varphi})_{,\varphi} = 0 \end{aligned} \quad (2.3)$$

The dimensionless boundary conditions referring to simple supports at  $\mu = 0$  and  $\mu = 1$  are

$$\begin{aligned} \frac{\partial^2 z}{\partial \mu^2} + \frac{\nu}{r^2} \frac{\partial^2 z}{\partial \varphi^2} = 0 \quad \frac{\partial^2 z}{\partial \mu \partial \varphi} = 0 \\ s \frac{\partial z}{\partial \tau} + s^2 \frac{\partial z}{\partial \mu} - n_x \frac{\partial z}{\partial \mu} - \frac{1}{r} n_{xy} \frac{\partial z}{\partial \varphi} + \frac{\partial^3 z}{\partial \mu^3} + \frac{1}{r^2} \frac{\partial^3 z}{\partial \mu \partial \varphi^2} = 0 \end{aligned} \quad (2.4)$$

The dimensionless boundary conditions referring to longitudinal free ends at  $\varphi = 0$  and  $\varphi = 1$  are

$$\begin{aligned} \frac{1}{r^2} \frac{\partial^2 z}{\partial \varphi^2} + \nu \frac{\partial^2 z}{\partial \mu^2} = 0 \quad \frac{\partial^2 z}{\partial \mu \partial \varphi} = 0 \\ \frac{1}{r} n_y \frac{\partial z}{\partial \varphi} + n_{xy} \frac{\partial z}{\partial \mu} - \frac{1}{r^3} \frac{\partial^3 z}{\partial \varphi^3} + \frac{1}{r} \frac{\partial^3 z}{\partial \mu^2 \partial \varphi} = 0 \end{aligned} \quad (2.5)$$

Partial differential equation (2.3) and boundary conditions (2.4), (2.5) constitute the mathematical model of the axially moving web with two simply supported and two free edges. The extended Galerkin method (Zienkiewicz and Morgan, 1983) is used to discretize the equation of motion and the boundary conditions. Comparison functions which satisfy all the boundary conditions are required for the classical Galerkin method, whereas the extended Galerkin method requires admissible functions that satisfy only the kinematic boundary conditions and not necessarily the natural boundary conditions.

The instantaneous deflection of the axially moving web at a point  $(\mu, \varphi)$  is assumed in the following form

$$z = \sum_{j=1}^{RS} A_j W_j(\mu, \varphi) f(\tau) = \mathbf{W}'\mathbf{T} \quad (2.6)$$

where  $A_j$  are scaling factors,  $f(\tau)$  – function of time,  $W_j(\mu, \varphi)$  – trial functions of the form

$$W_j = f_m(\mu) f_n(\varphi)$$

where  $m = 1, 2, 3, \dots, R$ ,  $n = 1, 2, 3, \dots, S$ ,  $j = (m - 1)S + n$ .

As the components of the trial functions, the modal functions  $f(\mu)$  for a simply supported beam and the modal functions  $f(\varphi)$  for a free-free beam were chosen

$$\begin{aligned} f_m(\mu) &= \sin(m\pi\mu) & m &= 1, 2, 3, \dots \\ f_1(\varphi) &= 1 \\ f_n(\varphi) &= \sinh[\varepsilon_n(1 - \varphi)] + \left[(-1)^n \frac{\sinh \varepsilon_n}{\sin \varepsilon_n}\right] \sin[\varepsilon_n(1 - \varphi)] & n &= 2, 4, 6, \dots \\ f_n(\varphi) &= \cosh[\varepsilon_n(1 - \varphi)] + \left[(-1)^n \frac{\sinh \varepsilon_n}{\sin \varepsilon_n}\right] \cos[\varepsilon_n(1 - \varphi)] & n &= 3, 5, 7, \dots \end{aligned} \quad (2.7)$$

where  $\varepsilon_n$  can be determined from

$$\tan(\varepsilon_n) + (-1)^{n+1} \varepsilon_n = 0 \quad n = 2, 3, 4, \dots \quad (2.8)$$

Figure 2 shows the plots of trial functions that have been assigned on the basis of formulas (2.7) and (2.6) for  $R = 3$ ,  $S = 3$ .

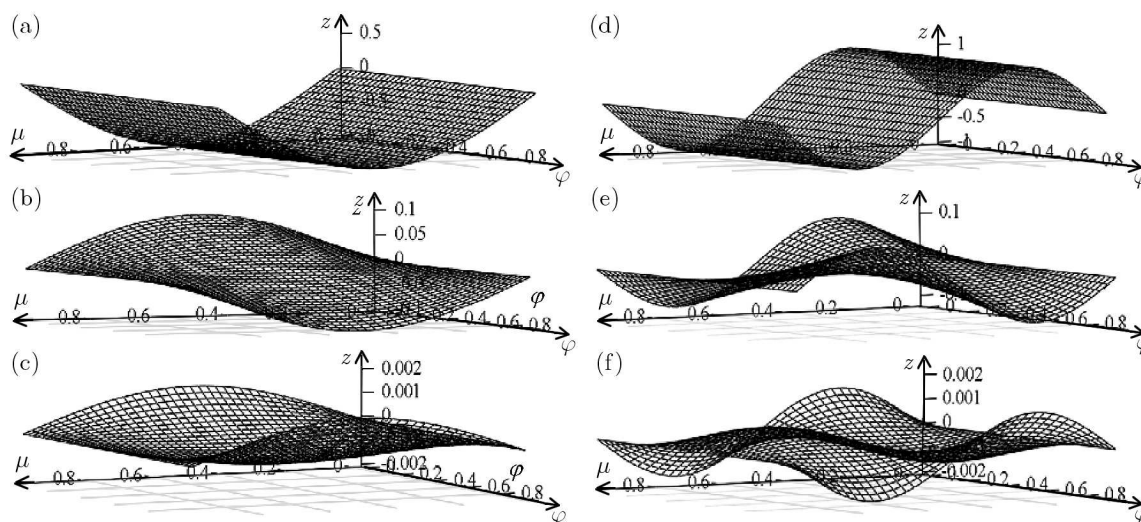


Fig. 2. Trial functions:  $W_{11}$  (a),  $W_{12}$  (b),  $W_{13}$  (c),  $W_{21}$  (d),  $W_{22}$  (e),  $W_{23}$  (f)

The governing equation is obtained by substituting the equation of motion, the boundary conditions and the trial functions into the extended Galerkin procedure. The weighting functions  $\psi_j$  are assumed to have the same form as the components of the trial functions. Then the governing equation can be rearranged into a matrix form

$$\mathbf{M}\ddot{\mathbf{T}} + \mathbf{G}\dot{\mathbf{T}} + \mathbf{K}\mathbf{T} = \mathbf{0} \quad (2.9)$$

where the elements of matrices are

$$\begin{aligned} M_{i,j} &= \int_0^1 \int_0^1 \psi_i W_j d\mu d\varphi & G_{i,j} &= \int_0^1 \int_0^1 2s\psi_i \frac{\partial W_j}{\partial \mu} d\mu d\varphi \\ K_{i,j} &= \int_0^1 \int_0^1 \left[ \left( \frac{\partial^2 \psi_i}{\partial \mu^2} + \frac{1}{r^2} \frac{\partial^2 \psi_i}{\partial \varphi^2} \right) \left( \frac{\partial^2 W_j}{\partial \mu^2} + \frac{1}{r^2} \frac{\partial^2 W_j}{\partial \varphi^2} \right) - s^2 \frac{\partial \psi_i}{\partial \mu} \frac{\partial W_j}{\partial \mu} \right. \\ &+ \frac{\partial \psi_i}{\partial \mu} \left( n_x \frac{\partial W_j}{\partial \mu} + n_{xy} \frac{1}{r} \frac{\partial W_j}{\partial \varphi} \right) + \frac{1}{r} \frac{\partial \psi_i}{\partial \varphi} \left( n_{xy} \frac{\partial W_j}{\partial \mu} + n_y \frac{1}{r} \frac{\partial W_j}{\partial \varphi} \right) \left. \right] d\mu d\varphi \\ &- (1 - \nu) \frac{1}{r^2} \int_0^1 \left( \psi_i \frac{\partial^3 w}{\partial \mu^2 \partial \varphi} + \frac{\partial \psi_i}{\partial \varphi} \frac{\partial^2 W}{\partial \mu^2} \right) \Big|_{\varphi=0}^1 d\mu = 0 \end{aligned} \quad (2.10)$$

Equation (2.9) was used for the investigations of dynamic behavior of the axially moving wide web.

### 3. Experimental stand and results of dynamic analysis

Using the mathematical model presented in Section 2, numerical studies of dynamic behavior of the moving web were carried out. The numerical results were verified experimentally on the lab stand shown in Fig. 3.

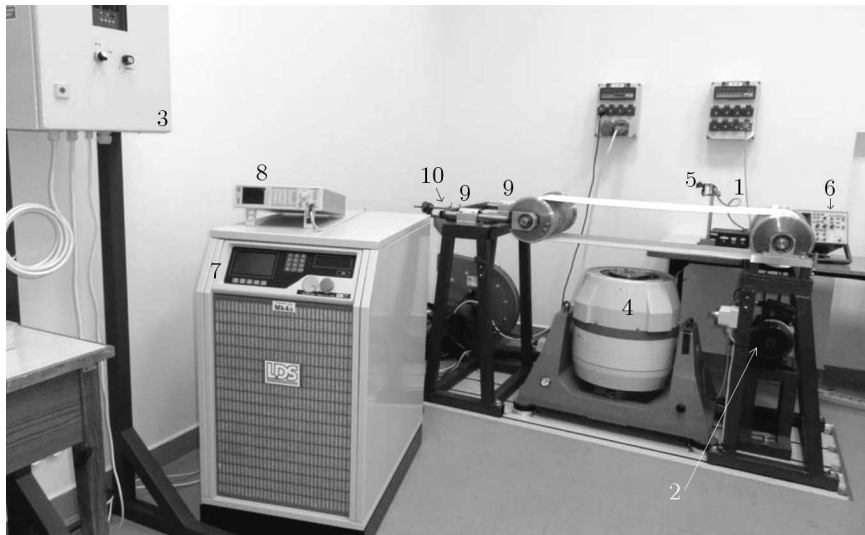


Fig. 3. Laboratory stand; 1 – composite web, 2 – drive motor, 3 – inverter; 4 – vibration exciter, 5 – laser optical sensor, 6 – oscilloscope HP 54600B, 7 – control of vibration exciter, 8 – frequency generator, 9 – thrust bearings, 10 – spring

The laboratory stand has the form of a belt transmission system. The right disc connected to the electric motor drives the web. Longitudinal tension in the web is controlled by tension

of the spring which is located in the support of the left disc. Micro-Epsilon ILD 1302-50 laser optical sensor was used to measure vibrations of the web. The object of the dynamic tests was a composite web consisting of a layer of fiber-reinforced polyurethane material. Physical parameters of the web material, geometrical dimensions and the results of calculations carried out on the basis of the tensile test are shown in Table 1.

**Table 1.** Parameters of the web material

No.	Parameters	Symbol	Value
1	Web thickness	$h$ [mm]	0.8
2	Web width	$b$ [m]	0.3
3	Total length of the web	$l$ [m]	2.62
3	Web density	$\rho$ [kg/m <sup>3</sup> ]	1100
4	Longitudinal modulus of elasticity	$E_x$ [N/m <sup>2</sup> ] – range 0.5-0.25% – range 3-6%	$0.378 \cdot 10^8$ $0.242 \cdot 10^8$
5	Transversal modulus of elasticity	$E_y$ [N/m <sup>2</sup> ] – range 0.5-0.25% – range 3-6%	$0.255 \cdot 10^8$ $0.169 \cdot 10^8$
6	Poisson number	$\nu$ [-]	0.5

The results of measurements of natural vibrations of the lower span under the longitudinal load 230 N/m are shown in Figs. 4-6. In any case a spectral graph corresponding to that vibrations obtained as a result of the FFT procedure is also presented.

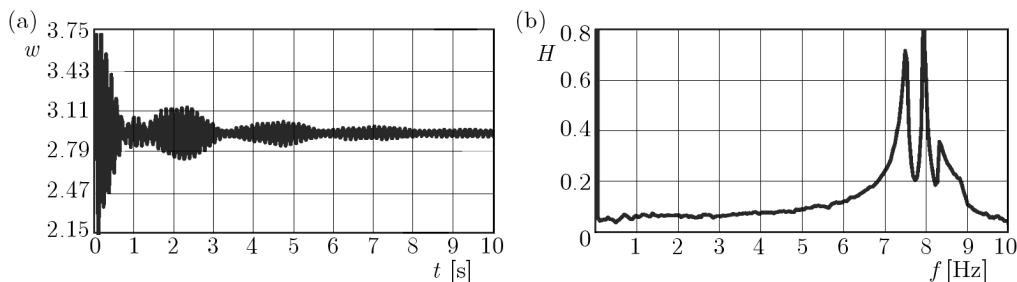


Fig. 4. Time history of free vibration (a) and FFT analysis (b);  $N_x = 230$  N/m,  $c = 0$

In the time history of vibrations in Fig. 4a beat phenomenon is visible. The beating makes three natural frequencies appear as close peaks in the spectrum plot in Fig. 4b. When the web transport speed increases, the values of free vibration frequencies decrease. This phenomenon is illustrated by the graphs in Fig. 5, for the transport speed  $c = 3.7$  m/s.

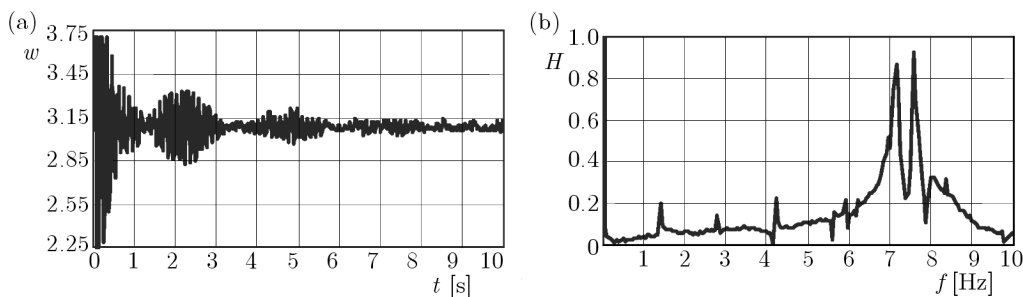


Fig. 5. Time history of free vibration (a) and FFT analysis (b);  $N_x = 230$  N/m,  $c = 3.7$  m/s

Figure 5b also shows narrower peaks representing forced vibrations with frequencies that are multiples of the fundamental frequency  $f = 1.4$  Hz. Forced vibrations came from a change in

the transport speed due to the connection zone of web with the length 295 mm characterized by a greater thickness than the rest of the web. When the web transport speed increases, the values of forced vibration frequencies increase as well. At such transport speeds of the web, in which the natural frequencies coincide with the successive multiples of the fundamental frequency of vibration excitation, resonances occurs. In Fig. 6, at the transport speed  $c = 11.1$  m/s, the web enters the zone of the primary resonance. Then the lowest natural frequency  $f_1 = 4.3$  Hz is equal to the lowest frequency of excitation. In the spectrum plot at the frequency 3.2 Hz, a small peak is visible, which comes from motion of the end of the connection zone.

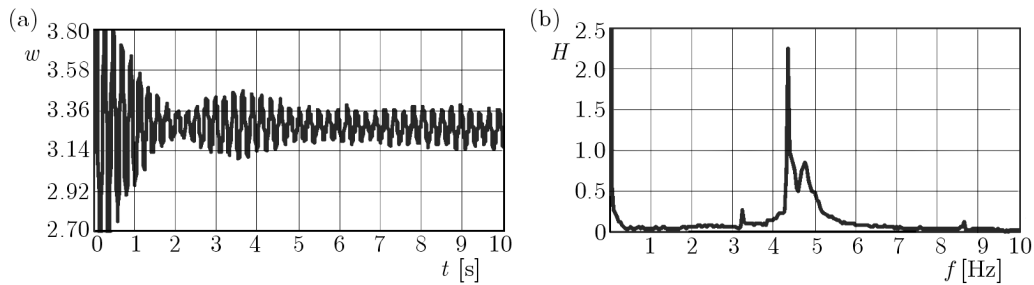


Fig. 6. Time history of free vibration (a) and FFT analysis (b);  $N_x = 230$  N/m,  $c = 11.1$  m/s

All measurement results of natural and forced frequencies of vibration of the moving web in the lower span in the speed range  $c = 0-15$  m/s under the load  $N_x = 230$  N/m are shown in Fig. 7.

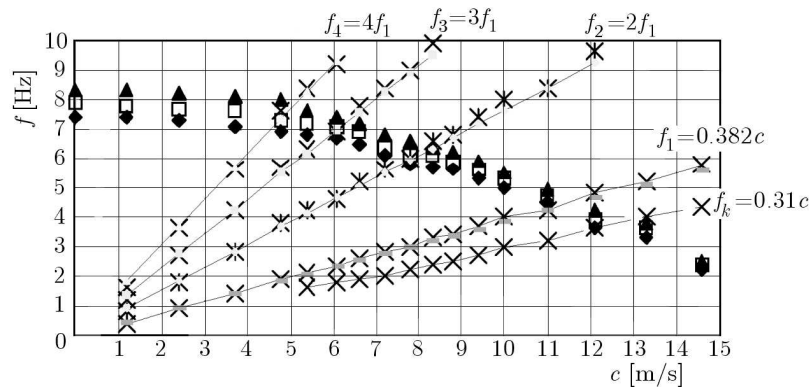


Fig. 7. Measurements results of natural and forced frequencies of the moving web;  $N_x = 230$  N/m, ( $\diamond, \square, \blacktriangle$ ) – natural frequencies, ( $\times$ ) –forced frequencies)

In Fig. 7, theoretical values of lowest multiplies of the fundamental exciting frequency are marked with solid lines. The experimental results presented in Fig. 7 were compared with the results of numerical calculations of natural frequencies using the mathematical model shown in the second section. The results of comparative tests are shown in Fig. 8.

#### 4. Conclusions

Theoretical-experimental dynamic analysis of an axially moving wide composite web is presented in this paper. The mathematical model of the system under consideration, derived earlier by the co-author, has the form of a differential equation with partial derivatives. Mathematical complication of this equation makes it impossible to determine the exact solutions of this model. The approximate solution using the extended Galerkin method has been determined in this work. To describe deflection of the web, the extended Galerkin method enables making use of functions

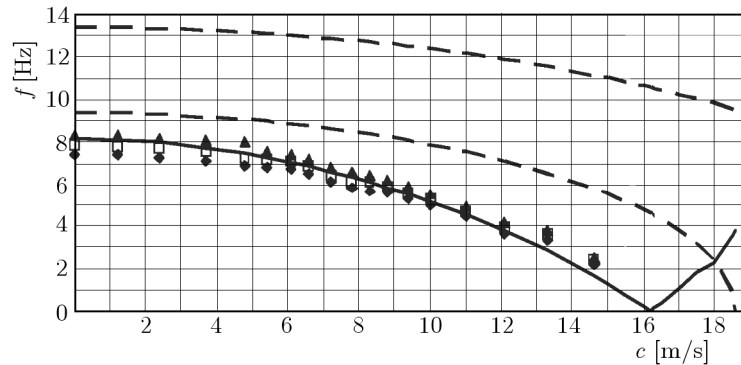


Fig. 8. Comparison of experimental measurements with theoretical calculations of natural frequencies;  $N_x = 230 \text{ N/m}$ , ( $\diamond$ ,  $\square$ ,  $\blacktriangle$ ) – measured frequencies, (—) – results of calculations of bending frequencies, (---) – results of calculations of torsional frequencies

that do not fully satisfy all boundary conditions. Dynamic analysis of the mathematical model allowed determination of the natural frequency of bending and torsional vibrations of the axially moving web.

Experimental investigations of dynamic behavior of the axially moving web was performed on a laboratory stand in form of a belt transmission system, in which the web in form of a loop was placed between two conducting shafts. A laser optical sensor was used to measure vibration of the web. For web tension considered in the experimental studies of transverse vibrations, a beating phenomenon occurred. The beating caused three natural frequencies to appear close to each other. When the web transport speed increased, the values of free vibration frequencies decreased. On the other hand, motion of the connection zone of the web, characterized by a greater thickness than the rest of the web, forced vibrations of the system. The forced vibration frequency increased with increasing transport speed of the web. While changing the transport speed, the resonance occurred when the natural frequency levelled with the successive multiples of the excitation frequency. After passing the main resonance zone, the web passed to a new equilibrium position around which natural vibrations took place.

The experimental verification of the numerical studies concerned the lowest frequencies of bending and torsional vibrations. Accuracy with which the frequency was numerically determined depended mainly on the accuracy of determination of the web tension. The fundamental frequency of bending vibration was determined numerically with the greatest accuracy.

## References

1. CHEN L.-Q., YANG X.-D., CHENG C.-J., 2004, Dynamic stability of an axially moving viscoelastic beam, *European Journal of Mechanics A/Solids*, **23**, 659-666
2. FUNG R.-F., HUANG J.-S., CHEN Y.-C., 1997, The transient amplitude of the viscoelastic traveling string: an integral constitutive law, *Journal of Sound and Vibration*, **201**, 2, 153-167
3. HATAMI S., AZHARI M., SAADATPOUR M.M., 2007, Free vibration of moving laminated composite plates, *Composite Structures*, **80**, 609-620
4. HATAMI S., RONAGH H.R., AZHARI M., 2008, Exact free vibration analysis of axially moving viscoelastic plates, *Composite Structures*, **86**, 1738-1746
5. KIM J., CHO J., LEE U., PARK S., 2003, Modal spectral element formulation for axially moving plates subjected to in-plane axial tension, *Computers and Structures*, **81**, 2011-2020
6. LIN C.C., 1997, Stability and vibration characteristics of axially moving plates, *International Journal of Solid and Structures*, **34**, 24, 3179-3190



7. MARYNOWSKI K., 2006, Two-dimensional rheological element in modeling of axially moving viscoelastic web, *European Journal of Mechanics A/Solids*, **25**, 729-744
8. MARYNOWSKI K., 2008, *Dynamics of the Axially Moving Orthotropic Web*, Springer Verlag
9. MARYNOWSKI K., 2010, Free vibration analysis of the axially moving Levy-type viscoelastic plate, *European Journal of Mechanics A/Solids*, **29**, 879-886
10. MARYNOWSKI K., KAPITANIAK T., 2007, Zener internal damping in modeling of axially moving viscoelastic beam with time-dependent tension., *International Journal of Non-Linear Mechanics*, **42**, 1, 118-131
11. SACK R.A., 1954, Transverse oscillations in travelling strings, *British Journal of Applied Physics*, **5**, 224-226
12. ULSOY A.G., MOTE C.D. JR., 1982, Vibrations of wide band saw blades, *Journal of Eng. Industr. ASME*, **104**, 1, 71-78
13. WANG X., 1999, Numerical analysis of moving orthotropic thin plates, *Computers and Structures*, **70**, 467-486
14. YANG X.-D., CHEN L.-Q., 2005, Bifurcation and chaos of an axially accelerating viscoelastic beam, *Chaos, Solutions and Fractals*, **23**, 1, 249-258
15. ZIENKIEWICZ O.C., MORGAN K., 1983, *Finite Elements and Approximation*, Wiley, New York

### Dynamika szerokiej wstęgi przesuwanej się osiowo

#### Streszczenie

W pracy przedstawiono teoretyczno-doświadczalną analizę dynamiczną przesuwanej się osiowo szerokiej kompozytowej wstęgi. Model matematyczny rozpatrywanego układu ma postać równania różniczkowego o pochodnych cząstkowych. Przybliżone rozwiązanie modelu matematycznego zostało określone przy wykorzystaniu rozszerzonej metody Galerkin. Analiza dynamiczna umożliwia wyznaczenie częstotliwości drgań własnych giętych i skrętnych wstęgi. Badania eksperymentalne dynamiki przesuwanej się osiowo wstęgi zostały przeprowadzone na stanowisku laboratoryjnym w postaci przekładni pasowej. Eksperymentalna weryfikacja badań numerycznych dotyczyła wyznaczenia najniższych częstotliwości drgań giętych i skrętnych wstęgi. Podstawowa częstotliwość drgań giętych została wyznaczona w badaniach numerycznych z największą dokładnością.

*Manuscript received October 10, 2011; accepted for print November 17, 2011*